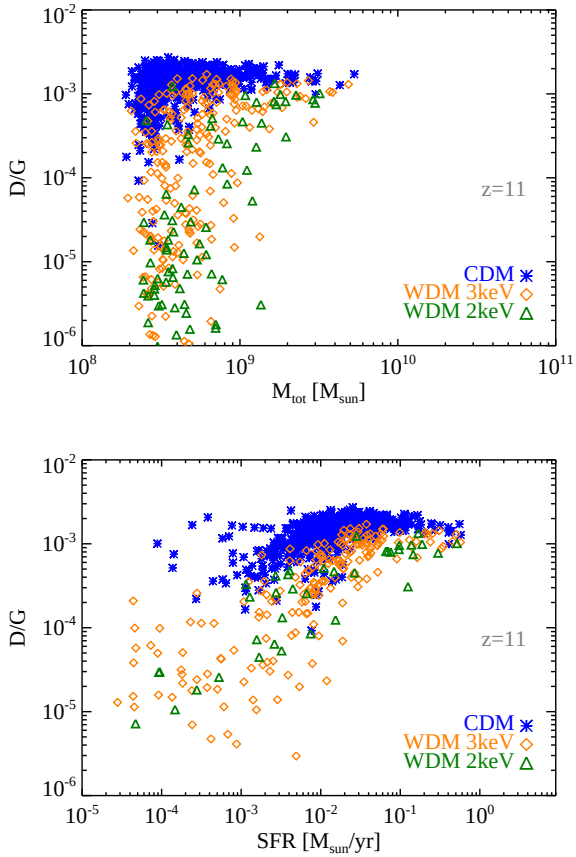

Fig. 6. Expected dust-to-gas ratios, D/G, as a function of the total halo mass for galaxies in the CDM, 3 keV WDM, and 2 keV WDM fiducial runs (top) and corresponding relation with the local SFR (bottom).

Adams et al. 2023; Finkelstein et al. 2022; Donnan et al. 2023). Since the observed samples are affected by completeness issues, cosmological stellar-mass values shall be considered as lower limits for the actual ones. By comparing JWST-inferred $\Omega_\star$ data and simulation data, we see a generally increasing trend with time, as a consequence of cosmological structure growth (and consistently with the SFRD shown in Fig. 2). There are obvious differences in the high-redshift ($z \gtrsim 10$) window. While both fiducial and basic CDM simulation results are consistent with JWST data, 2 keV WDM values are below all the $z \gtrsim 9.5$ lower limits, independently of the details of the physical implementation or resolution. This is in tension with WDM with particle masses $m_{\rm WDM} \lesssim 2$ keV. For the 3 keV WDM case it is not possible to give definitive assessments, with any conclusion being degenerate with the uncertainties on stellar masses at high z (Santini et al. 2023; Finkelstein et al. 2022).

A complementary point of view is given by the redshift evolution of the H_2 mass density (ρ_{H_2}) parameter $\Omega_{H_2} = \rho_{H_2}/\rho_{0,\rm crit}$ for the different dark-matter models and compared to available constraints at $z \simeq 6$–7 (Riechers et al. 2020), in the right panel of the figure. We note that H_2 is a powerful tracer of primordial structure formation and a major indicator of cold-gas collapse at all cosmic epochs. Since it is very sensitive to several physical and chemical processes (gas thermal state, chemical composition, dust content), its investigation is useful to understand the origin of primordial galaxies and rule out non-performing models. As it is clear from the trends, the fiducial CDM and 3 keV WDM results are in line with VLA constraints, while the 2 keV WDM scenario under-predicts Ω_{H_2}. For all the models considered Ω_{H_2} evolution is very similar at $z \gtrsim 14$, as cosmic gas has not formed significant amounts of molecules yet, and star formation can take place only in a few (larger at the time) haloes. While the growth of cosmic structures proceed, more and more gas condenses and forms H_2, as is visible from the Ω_{H_2} behaviour at lower z.

It is important to stress that the conclusions about CDM and WDM are based on the detailed implementation employed here. A simpler (basic) modelling would suggest misleading results, with smaller Ω_{H_2} values for all dark-matter scenarios and for any $z \gtrsim 7$. The plot also highlights that changes due to an improved description can be comparable to or larger than the ones induced by a finer resolution, as results, for example, from the trends in the basic, fiducial, and HR CDM/WDM runs.

Finally, we briefly discuss a couple of possible probes that, in the future, might help disentangle the nature of dark matter. Information about CDM and WDM implications for cosmic structures could be given by the overall evolution of the cumulative number counts of stellar (potentially visible) objects with mass above a fixed threshold. In Fig. 8 we show predicted simulation results in the fiducial CDM and WDM runs for two different stellar-mass thresholds: $10^7\,M_\odot/h$ and $10^4\,M_\odot/h$. As is visible in the figure, the discrepancies of galaxy counts are of about 1 dex at $z \gtrsim 10$ when a minimum stellar-mass threshold of $10^7\,M_\odot/h$ is assumed (left panel) and reach 2 dex when a more extreme threshold of $10^4\,M_\odot/h$ is considered (right panel). At lower z, differences are smaller, but they can persist down to $z \simeq 6$. In the future, once more data will have been collected by JWST and other upcoming facilities, it will be possible to pose more stringent limits, possibly at fraction of keV levels, on different scenarios by exploiting such trends.

Another interesting opportunity to pose constraints on dark matter is linked to the observable signatures of early CO emission. We note that CO is a strong emitter of galactic gas and its signal has been detected up to $z \simeq 7$ (with e.g., ALMA, VLA, NOEMA, etc.). In Fig. 9 we show the expected CO luminosity, $L_{\rm CO}$, as a function of the halo total mass, derived for CDM, 3 keV WDM, and 2 keV WDM cosmologies according to Bolatto et al. (2013). For the sake of clarity, we only considered the galaxy populations expected in the fiducial runs at $z \simeq 7.3$, 9, and 11. The general behaviour is similar in all the models, with scattered points at lower masses ($\lesssim 10^9\,M_\odot$) and a roughly linear trend as an upper limit. The scatter is due to the buildup of the molecular content in the haloes that are just hosting gas collapse and primordial star formation, while more evolved structures have already converted a significant fraction of atomic gas into molecules. The latter delimits the $L_{\rm CO}$-mass relation, which holds for both CDM and WDM galaxies. Although the physical process is qualitatively the same, typical timescales change. Indeed, spectral suppression in WDM scenarios induces delays in halo formation and cosmic-gas collapse, during which molecules are formed. So, the resulting $L_{\rm CO}$ signal is tightly bound to the underlying nature of dark matter and the impacts of CDM versus WDM are particularly visible at early times. WDM small-scale suppression is recognizable at $z \gtrsim 9$, when, below $10^9\,M_\odot$, there is a deficit in the expected $L_{\rm CO}$ emission up to a few dex (right panel at $z = 11$). At that time, CDM galaxies have already had enough time to complete molecule formation, while 2 keV WDM galaxies feature poorer number statistics and lower molecular content. The 3 keV WDM case expects galaxies that are in more advanced stages, but that have not reached the CDM ones, yet. By the first half billion years ($z = 9$, central panel), the trends start to converge and at $z = 7.3$ (left panel) different models are basically indistinguishable, since the original differences

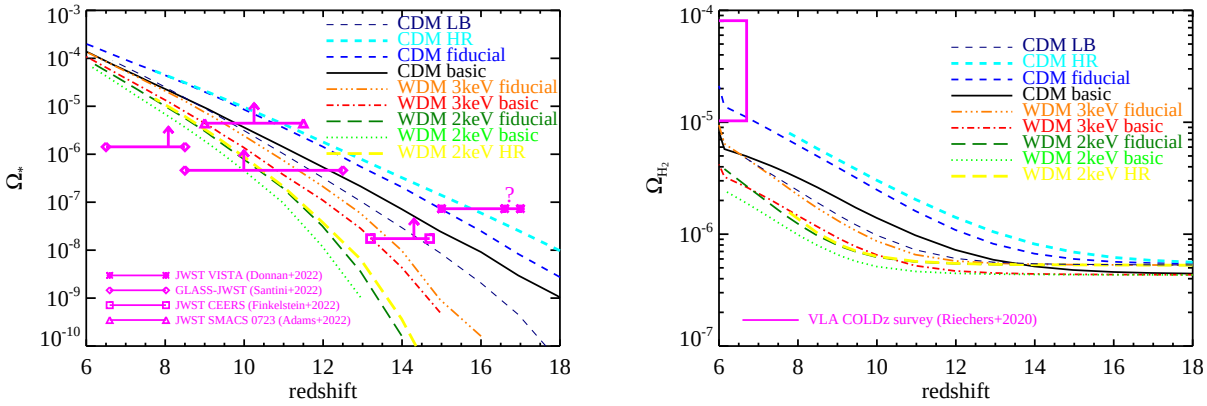

Fig. 7. Redshift evolution of the stellar-mass density parameter $\Omega_\star$ (left) for different models compared to JWST-inferred values and redshift evolution of the H_2 mass density parameter Ω_{H_2} (right) for different models compared to VLA COLDz data (magenta box).

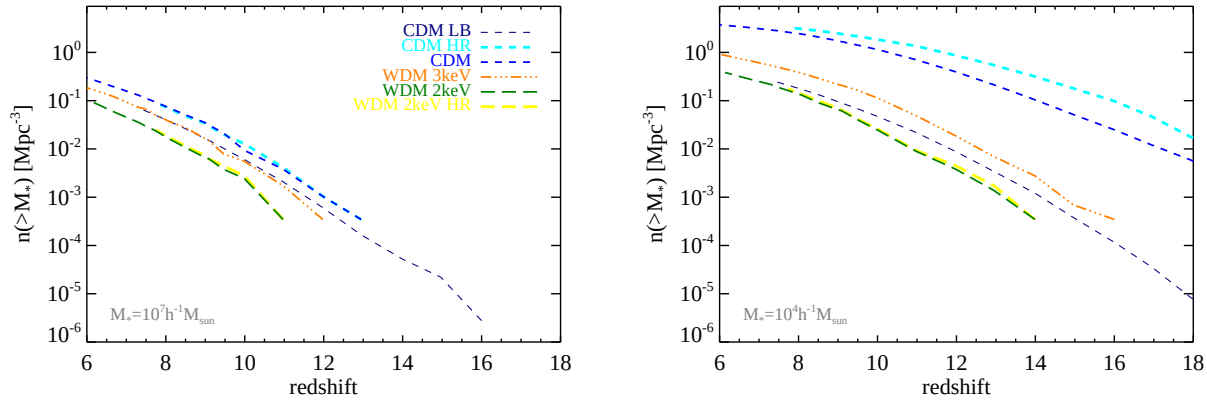

Fig. 8. Redshift evolution of the expected cumulative number density of objects with a minimum stellar mass of $10^7\,M_\odot/h$ (left) and $10^4\,M_\odot/h$ (right), for CDM, 3 keV WDM, and 2 keV WDM fiducial runs.

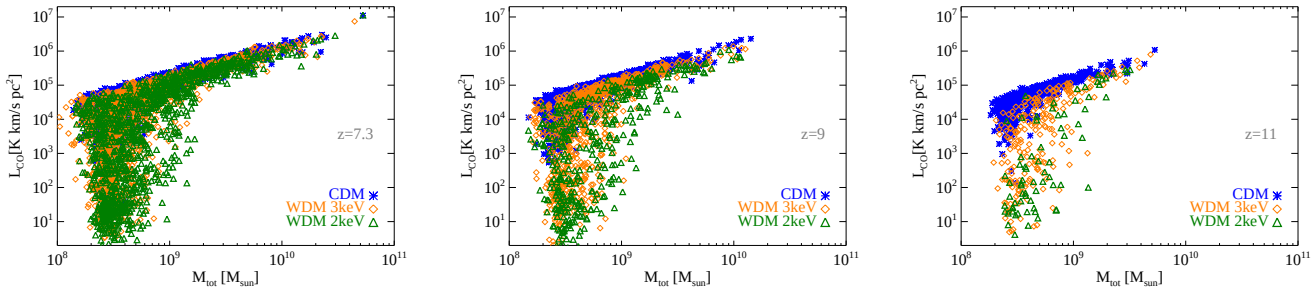

Fig. 9. Expected L_{CO} emission as function of the total halo mass in the CDM (asterisks), 3 keV WDM (squares), and 2 keV WDM (triangles) fiducial runs at $z = 7.3$ (left), $z = 9$ (centre), and $z = 11$ (right), respectively.

between CDM and WDM are erased by the ongoing feedback effects. This catchup takes place in only a few hundreds of million years. For this reason although challenging, tight constraints on the nature of dark matter might come through detection of CO emission at very early times.

4. Discussion and conclusions

In this work we have exploited the latest JWST observational determinations and novel up-to-date numerical simulations to put constraints on the nature of dark matter from high-redshift observations. We have compared the latest JWST-inferred high-z star formation estimates (Santini et al. 2023; Donnan et al. 2023; Finkelstein et al. 2022; Adams et al. 2023; Harikane et al. 2023; Bouwens et al. 2022) with a set of non-equilibrium hydrodynamical simulations which incorporate the new, rich, and accurate modelling of cosmic structure formation at early times by Maio et al. (2022). This attempt is the first one to try to set constraints on WDM by combining such modelling with state-of-the-art JWST observations at extremely high redshift. Previous works based on high-redshift hydro-simulations have either neglected a fully complete modelling of primordial gas and structures in CDM and WDM or had no or little data support for the primordial regimes probed by JWST.

We contrast galaxy buildup in the standard CDM model against two models with 2 and 3 keV WDM, respectively. We adopted cosmological matter density and expansion parameters that are consistent with both the standard

model and WMAP data. The latest *Planck* measurements (Planck Collaboration XVI 2014; Planck Collaboration VI 2020) suggest slightly different values, while spectral parameters are similar. This is an important point, because early structure formation and halo mass functions are mostly affected by variations in σ_8 which is consistently constrained by the aforementioned experiments. Thus, changing the initial parameter set does not lead to appreciable differences in our results and the overall trends are preserved (see also discussions in e.g., Maio et al. 2010, 2011a).

We generated initial conditions at high redshift via cosmological linear perturbation theory, which is well suited for such early regimes. Coherent supersonic flows of the baryons relative to the underlying dark-matter distribution on megaparsec scales are caused by higher-order corrections accounting for the advection of small-scale perturbations by large-scale velocity flows after decoupling. However, we have verified that, independently from the initial redshift (ranging between $z = 100$ and $z = 1020$), the implications of such bulk motions have no impact on the masses in the epoch studied in this work (Maio et al. 2011b).

As is typically done, we assumed that the statistical distribution of the primordial matter perturbation field is Gaussian. Deviations from Gaussianity could be present and could enhance or dampen the occurrence of objects with a given mass; nevertheless, the expected level of these primordial non-Gaussianities is so small that possible implications on molecular evolution, popIII and popII-I star formation, metal enrichment, gas temperature, and possibly detectable signals would be negligible and dominated by baryon effects (Maio & Iannuzzi 2011; Maio 2011; Maio & Khochfar 2012; Maio et al. 2012).

More critical uncertainties are about feedback processes and their degeneracies with the nature of dark matter. Fortunately, feedback effects usually have local impacts and alter the local chemical and physical properties of cosmic objects. Although their efficiency is poorly constrained, they play a significant role at low z, when structure evolution is in more advanced stages and possible dark-matter signatures have already been washed out (Schneider et al. 2014). Primordial galaxies are young structures and have experienced little feedback effects; therefore, their statistical occurrence is mainly driven by the underlying dark-matter model. For this reason, the early Universe is a precious window to test dark-matter models and, furthermore, calibrating feedback parameters in the low-z regime together with large high-z data samples might make it possible to both break the degeneracies and to provide hints on the late-time evolution of cosmic structures.

Predicted stellar and molecular mass density parameters, as well as star formation rate densities are consistent with early results of JWST data at $z \gtrsim 7$ and with previous VLA constraints at $z \simeq 7$ in the CDM and 3 keV WDM scenarios. JWST data do not show any hint of an excess of number densities of bright galaxies at $z \gtrsim 7$, compared to the standard model. Thus, current data are neither in tension with cold dark matter nor warm dark matter models with $m_{\rm WDM} > 2$ keV. Current data are mainly probing young, bright and rare objects, whose physical properties are remarkably similar in the different scenarios. Consistently with the short cosmic time of the infant Universe, these are expected to host little dust content. However, due to the low-mass power suppression, the faint end of the UV luminosity function flattens for lighter dark-matter particles, while the corresponding UV correlation function steepens significantly. These two different observables, especially when used in combination, can be extremely promising not only for constraining galaxy formation models (van Daalen et al. 2016), but also for disentangling dark-matter scenarios by using faint high-z visible sources. In the future, when more data for small, dim, high-z sources will be available, further hints may come from number density statistics and galactic CO emission luminosities.

Acknowledgements. We warmly thank the anonymous referee for his/her prompt feedback which helped us improve the manuscript and extend the original text with extremely constructive comments. UM acknowledges useful discussion with M. Castellano and is thankful to P. Santini and C. Donnan for sharing preliminary analysis of early JWST data. MV is supported by the PD51-INFN INDARK and ASI-INAF n. 2017-14-H.0 grants.

References

Adams, N. J., Conselice, C. J., Ferreira, L., et al. 2023, MNRAS, 518, 4755
Atek, H., Shuntov, M., Furtak, L. J., et al. 2023, MNRAS, 519, 1201
Barkana, R., Haiman, Z., & Ostriker, J. P. 2001, ApJ, 558, 482
Behroozi, P., & Silk, J. 2018, MNRAS, 477, 5382
Biagetti, M., Franciolini, G., & Riotto, A. 2023, ApJ, 944, 113
Bode, P., Ostriker, J. P., & Turok, N. 2001, ApJ, 556, 93
Bolatto, A. D., Wolfire, M., & Leroy, A. K. 2013, ARA&A, 51, 207
Bouwens, R., Illingworth, G., Oesch, P., et al. 2022, MNRAS, submitted, [arXiv:2212.06683]
Bowler, R. A. A., Jarvis, M. J., Dunlop, J. S., et al. 2020, MNRAS, 493, 2059
Boyarsky, A., Lesgourgues, J., Ruchayskiy, O., & Viel, M. 2009, JCAP, 05, 012
Boylan-Kolchin, M. 2022, ArXiv e-prints [arXiv:2208.01611]
Bruzual, G., & Charlot, S. 2003, MNRAS, 344, 1000
Carucci, I. P., & Corasaniti, P. -S. 2019, Phys. Rev. D, 99, 023518
Castellano, M., Fontana, A., Treu, T., et al. 2022, ApJ, 938, L15
Colin, P., Avila-Reese, V., & Valenzuela, O. 2000, ApJ, 542, 622
Corasaniti, P., Agarwal, S., Marsh, D., & Das, S. 2017, Phys. Rev. D, 95, 083512
Curti, M., D'Eugenio, F., Carniani, S., et al. 2023, MNRAS, 518, 425
Curtis-Lake, E., Carniani, S., Cameron, A., et al. 2022, Nat. Astron., submitted [arXiv:2212.04568]
Dayal, P., Mesinger, A., & Pacucci, F. 2015, ApJ, 806, 67
Donnan, C. T., McLeod, D. J., Dunlop, J. S., et al. 2023, MNRAS, 518, 6011
Ferrara, A., Pallottini, A., & Dayal, P. 2022, ArXiv e-prints [arXiv:2208.00720]
Finkelstein, S. L., Bagley, M. B., Haro, P. A., et al. 2022, ApJ, 940, L55
Furtak, L. J., Shuntov, M., Atek, H., et al. 2023, MNRAS, 519, 3064
Harikane, Y., Ouchi, M., Oguri, M., et al. 2023, ApJS, 265, 5
Haslbauer, M., Banik, I., Kroupa, P., Wittenburg, N., & Javanmardi, B. 2022, ApJ, 925, 183
Inayoshi, K., Harikane, Y., Inoue, A. K., Li, W., & Ho, L. C. 2022, ApJ, 938, L10
Iršič, V., Viel, M., Haehnelt, M. G., et al. 2017, Phys. Rev. D, 96, 023522
Kannan, R., Springel, V., Hernquist, L., et al. 2022, MNRAS, submitted [arXiv:2210.10066]
Kurmus, A., Bose, S., Lovell, M., et al. 2022, MNRAS, 516, 1524
Lapi, A., & Danese, L. 2015, JCAP, 2015, 003
Lapi, A., Ronconi, T., Boco, L., et al. 2022, Universe, 8, 476
Lewis, A., Challinor, A., & Lasenby, A. 2000, ApJ, 538, 473
Lovell, C. C., Harrison, I., Harikane, Y., Tacchella, S., & Wilkins, S. M. 2023, MNRAS, 518, 2511
Macciò, A. V., & Fontanot, F. 2010, MNRAS, 404, L16
Maio, U. 2011, CQG, 28, 225015
Maio, U., & Iannuzzi, F. 2011, MNRAS, 415, 3021
Maio, U., & Khochfar, S. 2012, MNRAS, 421, 1113
Maio, U., & Viel, M. 2015, MNRAS, 446, 2760
Maio, U., Dolag, K., Meneghetti, M., et al. 2006, MNRAS, 373, 869
Maio, U., Dolag, K., Ciardi, B., & Tornatore, L. 2007, MNRAS, 379, 963
Maio, U., Ciardi, B., Dolag, K., Tornatore, L., & Khochfar, S. 2010, MNRAS, 407, 1003
Maio, U., Khochfar, S., Johnson, J. L., & Ciardi, B. 2011a, MNRAS, 414, 1145
Maio, U., Koopmans, L. V. E., & Ciardi, B. 2011b, MNRAS, 412, L40
Maio, U., Salvaterra, R., Moscardini, L., & Ciardi, B. 2012, MNRAS, 426, 2078
Maio, U., Péroux, C., & Ciardi, B. 2022, A&A, 657, A47
Mason, C. A., Trenti, M., & Treu, T. 2023, MNRAS, 521, 497
Menci, N., Castellano, M., Santini, P., et al. 2023, ApJ, 938, L5
Naidu, R. P., Oesch, P. A., van Dokkum, P., et al. 2022a, ApJ, 940, L14
Naidu, R. P., Oesch, P. A., Setton, D. J., et al. 2022b, ApJL, submitted [arXiv:2208.02794]
Narayanan, V. K., Spergel, D. N., Dave, R., & Ma, C.-P. 2000, ApJ, 543, L103
Pacucci, F., Mesinger, A., & Haiman, Z. 2013, MNRAS, 435, L53
Palanque-Delabrouille, N., Yèche, C., Schöneberg, N., et al. 2020, JCAP, 2020, 038
Planck Collaboration VI. 2020, A&A, 641, A6

Planck Collaboration XVI. 2014, A&A, 571, A16
Reed, D. S., Bower, R., Frenk, C. S., Jenkins, A., & Theuns, T. 2007, MNRAS, 374, 2
Riechers, D. A., Hodge, J. A., Pavesi, R., et al. 2020, ApJ, 895, 81
Rodighiero, G., Bisigello, L., Iani, E., et al. 2023, MNRAS, 518, L19
Rudakovskyi, A., Mesinger, A., Savchenko, D., & Gillet, N. 2021, MNRAS, 507, 3046
Santini, P., Fontana, A., Castellano, M., et al. 2023, ApJ, 942, L27
Schneider, A., Anderhalden, D., Macciò, A. V., & Diemand, J. 2014, MNRAS, 441, L6
Springel, V. 2005, MNRAS, 364, 1105
Stefanon, M., Bouwens, R. J., Labbé, I., et al. 2021, ApJ, 922, 29
Tornatore, L., Borgani, S., Dolag, K., & Matteucci, F. 2007, MNRAS, 382, 1050
Treu, T., Roberts-Borsani, G., Bradac, M., et al. 2022, ApJ, 935, 110
van Daalen, M. P., Henriques, B. M. B., Angulo, R. E., & White, S. D. M. 2016, MNRAS, 458, 934
Viel, M., Lesgourgues, J., Haehnelt, M. G., Matarrese, S., & Riotto, A. 2005, Phys. Rev. D, 71, 063534
Viel, M., Becker, G. D., Bolton, J. S., & Haehnelt, M. G. 2013, Phys. Rev. D, 88, 043502